

Evidence for large electric polarization from collinear commensurate magnetism in multiferroic TmMnO_3

V Yu Pomjakushin¹, M Kenzelmann^{1,2}, A Dönni³, A B Harris⁴, T Nakajima⁵, S Mitsuda⁵, M Tachibana³, L Keller¹, J Mesot¹, H Kitazawa³ and E Takayama-Muromachi³

¹ Laboratory for Neutron Scattering, ETH Zürich & Paul Scherrer Institute, CH-5232 Villigen, Switzerland

² Laboratory for Solid State Physics, ETH Zürich, CH-8093 Zürich, Switzerland

³ National Institute for Materials Science (NIMS), 1-2-1 Sengen, Tsukuba, Ibaraki 305-0047, Japan

⁴ Department of Physics and Astronomy, University of Pennsylvania, Philadelphia, PA 19104, USA

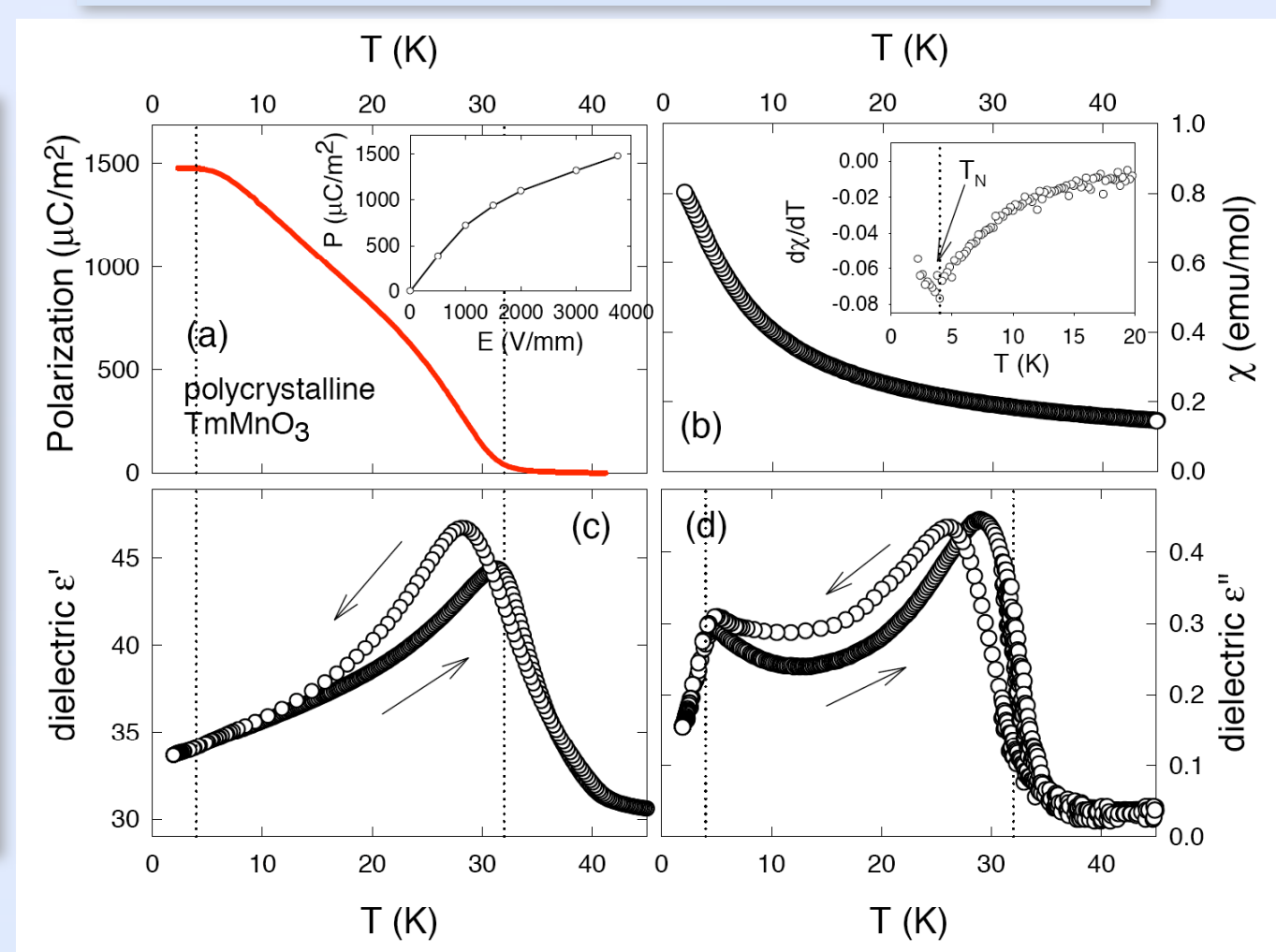
⁵ Department of Physics, Faculty of Science, Tokyo University of Science, Kagurazaka 1-3, Shinjuku-ku, Tokyo, Japan

There has been tremendous research activity in the field of magneto-electric (ME) multiferroics after Kimura et al (2003 Nature 426 55) showed that antiferromagnetic and ferroelectric orders coexist in orthorhombically distorted perovskite TbMnO_3 and are strongly coupled. It is now generally accepted that ferroelectricity in TbMnO_3 is induced by magnetic long-range order that breaks the symmetry of the crystal and creates a polar axis (Kenzelmann et al 2005 Phys. Rev. Lett. 95 087206). One remaining key question is whether magnetic order can induce ferroelectric polarization that is as large as that of technologically useful materials. We show that ferroelectricity in orthorhombic (o) TmMnO_3 is induced by collinear magnetic order, and that the lower limit for its electric polarization is larger than in previously investigated orthorhombic heavy rare-earth manganites. The temperature dependence of the lattice constants provides further evidence of large spin-lattice coupling effects. Our experiments suggest that the ferroelectric polarization in the orthorhombic perovskites with commensurate magnetic ground states could pass the $5000 \mu\text{C m}^{-2}$ threshold, as predicted by theory (Sergienko et al 2006 Phys. Rev. Lett. 97 227204; Picozzi et al 2007 Phys. Rev. Lett. 99 227201).

New Journal of Physics **11**, 043019 (2009)

Temperature dependences

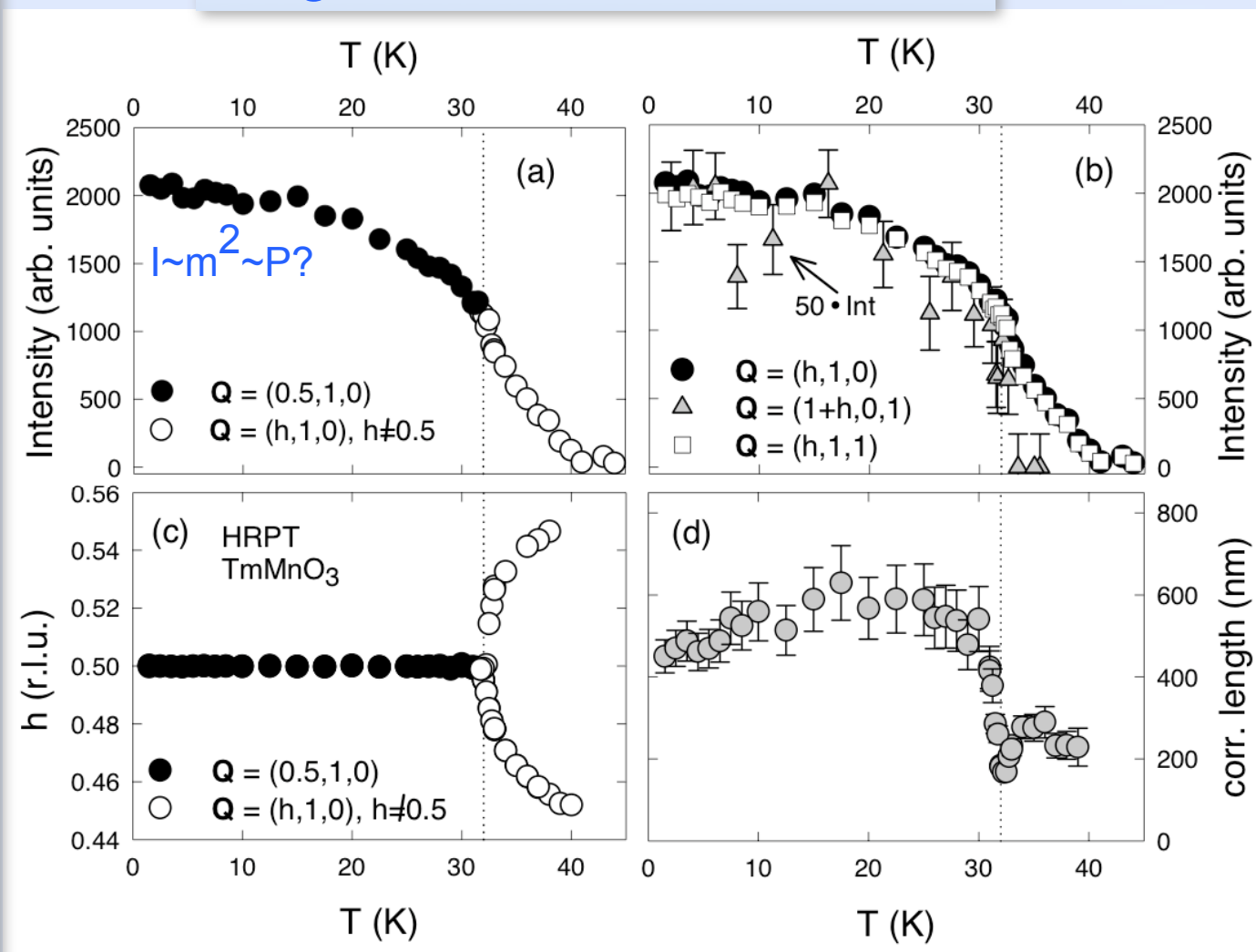
Magnetic and electric susceptibilities



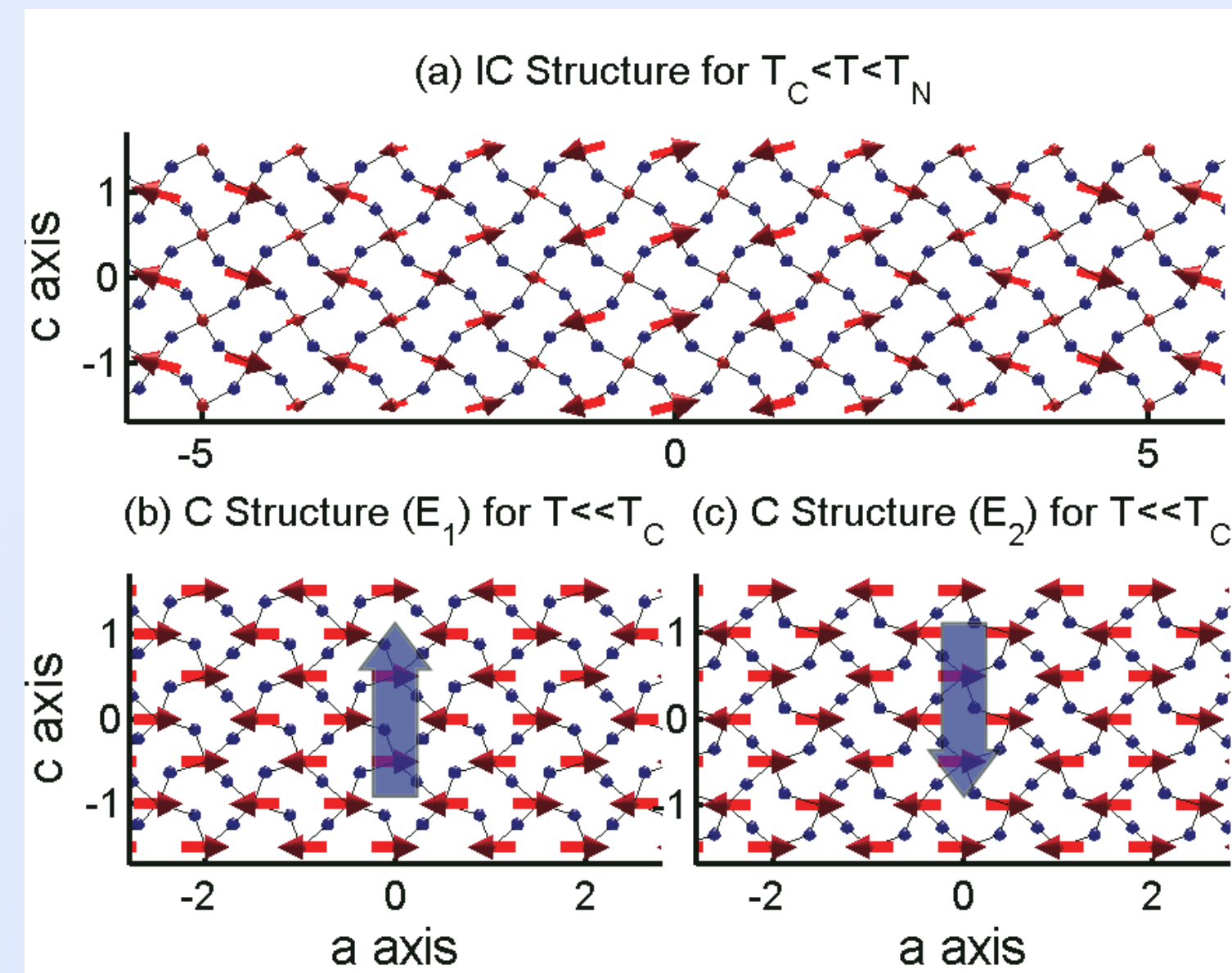
(a) Electric polarization of a pressed powder sample determined using pyroelectric measurements after cooling an electrically poled sample. (b) Magnetic susceptibility (c) Real and (d) imaginary part of the dielectric susceptibility measured at a frequency of $f=100\text{kHz}$

(a) magnetic Bragg peak intensity at $Q=(0.5,1,0)$ in the commensurate phase, or the added intensities at $Q=(\pm q, 1, 0)$ for $0.45 < q < 0.5$. (b) Comparison of different magnetic peaks, showing that they have the same temperature dependence in commensurate phase. The $Q=(1.5,0,1)$ peak is only present in the commensurate phase, and is evidence of the ordering of Tm^{3+} spins. (c) a-component of k-vector (d) magnetic correlation length as deduced from the width of the magnetic Bragg peaks.

Magnetic neutron diffraction

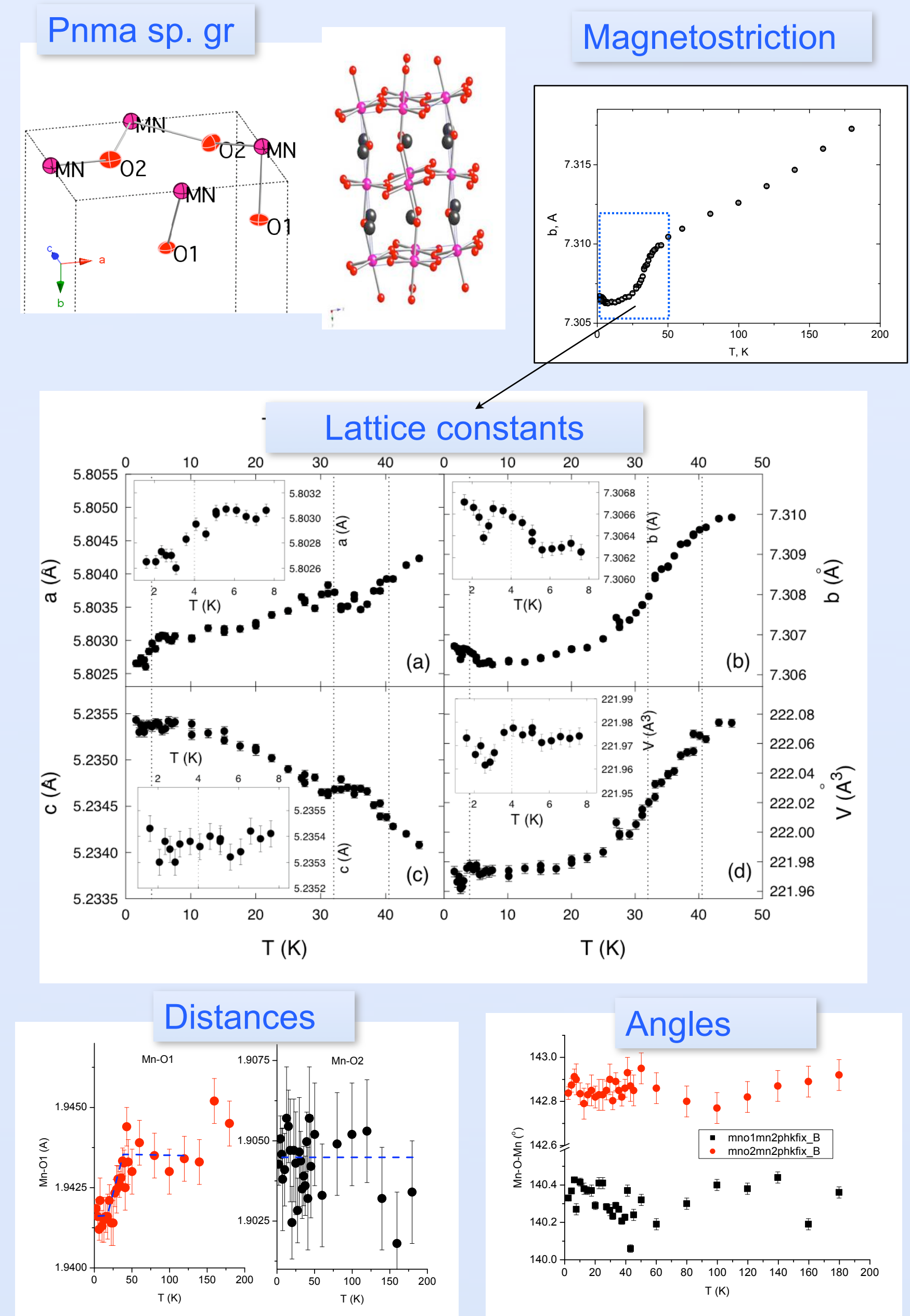


Magnetic structure Electric polarization



Chemical structure of showing Mn in red and O in blue. (a) Incommensurate amplitude-modulated Mn^{3+} spin order in the paraelectric phase for $32 \text{ K} < T < 40 \text{ K}$. (b-c) Commensurate Mn^{3+} spin order of E_1 and E_2 type, respectively, in the ferroelectric phase for $T << 32 \text{ K}$ (symmetry: 2D-irrep τ_1 , Kovalev). The large arrows show the direction of the spontaneous polarization along the c-axis (polar vector for irrep τ_1 is allowed along a and c) that can arise, for example, from a movement of the Mn^{3+} and O^{2-} positions (shown here schematically) to adjust the Mn-O-Mn angle for parallel and antiparallel nearest-neighbor alignment, thereby lowering symmetry through the creation of a polar axis. (a-c) The moments in the neighboring planes along y-axis are oriented in the opposite direction.

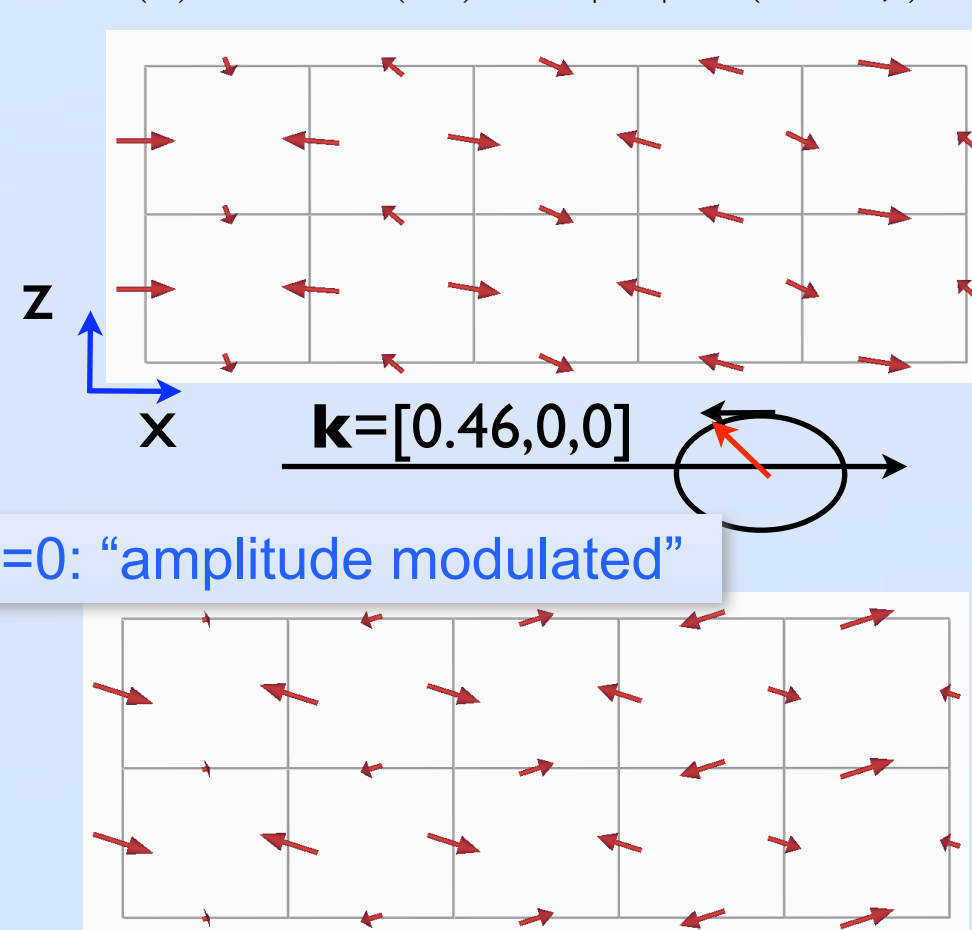
Crystal structure



Propagation of spin

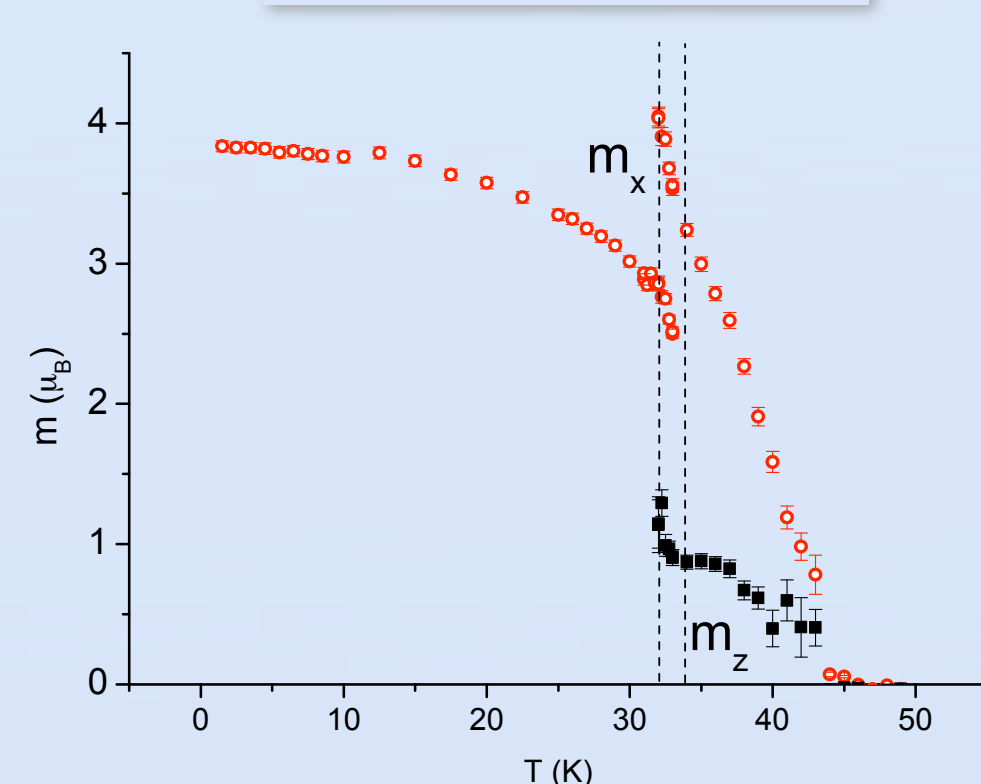
for arbitrary φ : both direction and size of S_1 are changed

$$S_1(x) = C_1 \cos(kx)e_x + |C_3| \cos(kx + \varphi)e_z$$

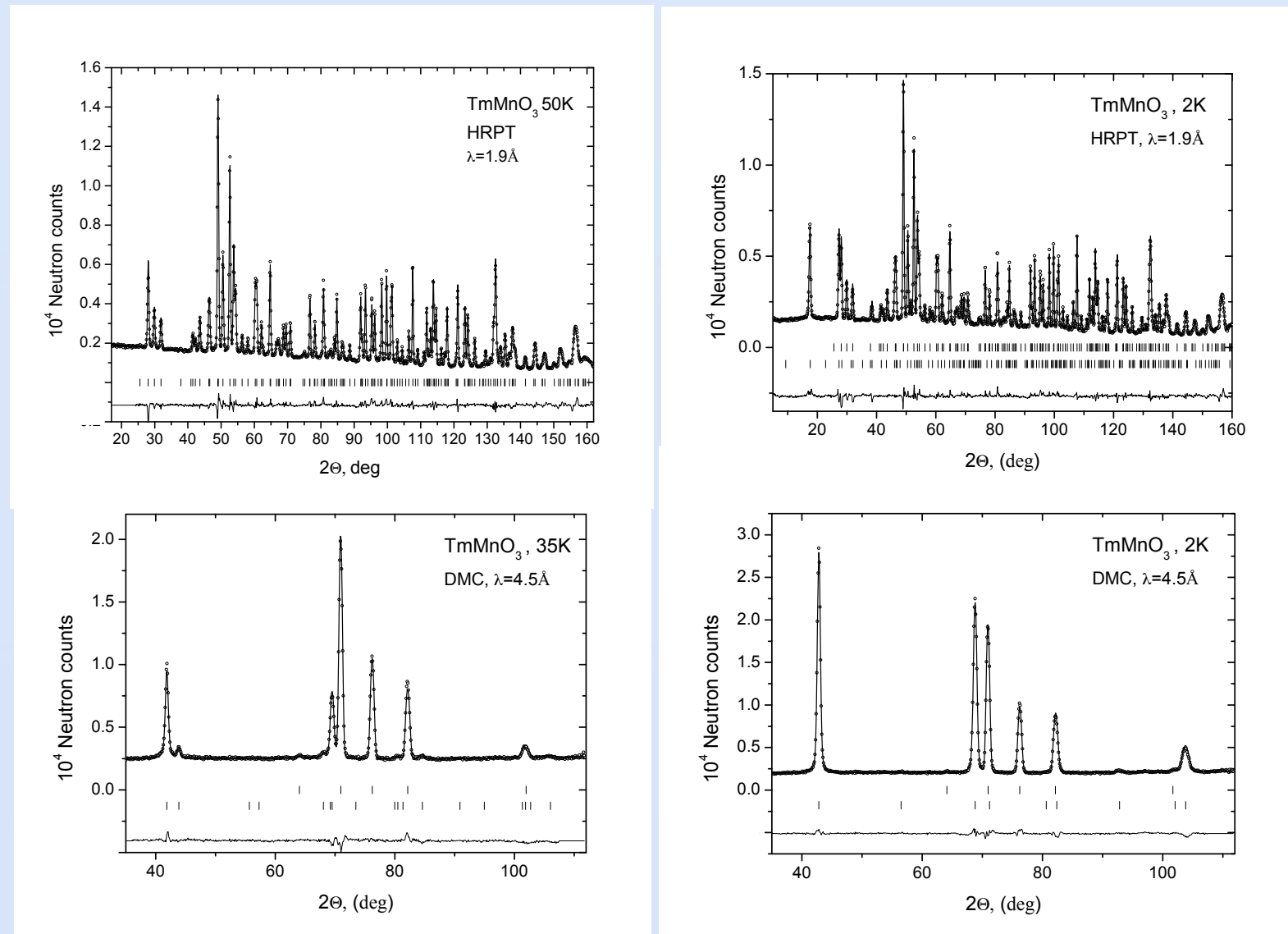


$\varphi=0$: "amplitude modulated"

Magnetic moment/ fourier component



Patterns, 1.9Å HRPT and 4.5Å DMC



Symmetry adapted b. f.

Pnma, no.62: 8 symmetry operators
 (1) 1, (2) 2(0,0,1/2)±,0,z, (3) 2(0,1,0) 0,y,0, (4) 2(1/2,0,0) x,1/2, (5) 1 0,0,0, (6) a x,1/2, (7) m x,1,z, (8) n(0,1/2) 1/2,y,2
 $k = \begin{bmatrix} 1 \\ 0 \\ 0 \end{bmatrix}$ Kovalev: k_2, T_85 : two 2D irreps $k = \begin{bmatrix} q \\ 0 \\ 0 \end{bmatrix}$ Kovalev: k_7, T_30 : four 1D irreps
Mn (0,0,1/2), axial: $3\tau_1^{1D} \oplus 3\tau_2^{1D}$ $3\tau_1 \oplus 3\tau_2 \oplus 3\tau_3 \oplus 3\tau_4$
 (1) $1, h_1$ (4) $2_x, h_2$ (7) m_y, h_{27} (6) m_z, h_{28}
 $0, 0, \frac{1}{2}$ $\frac{1}{2}, \frac{1}{2}, 0$ $0, \frac{1}{2}, \frac{1}{2}$ $\frac{1}{2}, 0, 0$
 Six basis functions for $3\tau_1^{1D}$
 h_1 h_2 h_{27} h_{28}
 ψ_{1x} 1 1 -1 -1
 ψ_{2y} 1 -1 1 -1
 ψ_{3z} 1 -1 -1 1
 ψ_{4x} 1 -1 -1 1
 ψ_{5y} 1 1 1 1
 ψ_{6z} 1 1 -1 -1
 Best fit: equivalent solutions E_1, E_2
 $M_{\text{Mn}} \parallel x$
 Three basis functions for $3\tau_2^{1D}$
 h_1 h_2 h_{27} h_{28}
 ψ_{1x} 1 -a -1 a
 ψ_{2y} 1 a 1 a
 ψ_{3z} 1 a -1 a
 where $a = e^{-\pi i q}$
 Best fit: $C_1 \psi_{1x} + C_3 \psi_{3z}$
 cycloid
 $k = \begin{bmatrix} q \\ 0 \\ 0 \end{bmatrix}$
Tm (x,1/4,z), axial: $2\tau_1^{2D} \oplus 4\tau_2^{2D}$
 $2\tau_1^{2D}$: all basis functions $\parallel y$
 Best fit: is not for τ_1 but for τ_2 with $M_{\text{Tm}} \parallel z$